AD-A158 693 EMITTANCE MEASUREMENTS OF SPACE CHARGE DOMINATED ELECTRON BEAM(U) NAVAL SURFACE WEAPONS CENTER SILVER SPRING MD W NAMKUNG ET AL. 01 JUN 85 NSWC/TR-85-244 1/1

UNCLASSIFIED F/G 20/7 NL

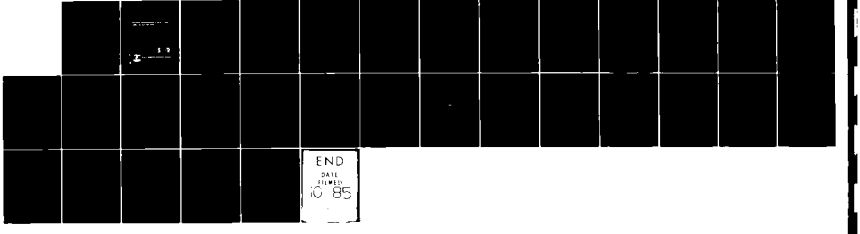

END
DATE FILMED
10 85

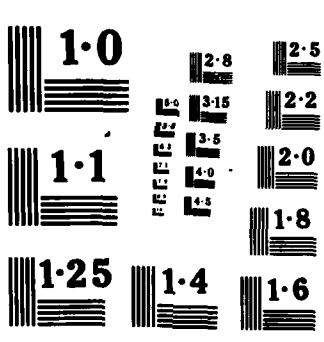
1·0
1·1
1·25
1·4
1·6
1·8
2·0
2·2
2·5
2·8
3·15
3·5
4·0
4·5

AD-A158 693

[redacted]

BY WON HAMKUNG [redacted]

RESEARCH AND TECHNOLOGY DEPARTMENT

[redacted]

[redacted]

DTIC
[redacted]

UNCLASSIFIED

SECURITY CLASSIFICATION OF THIS PAGE *(When Data Entered)*

REPORT DOCUMENTATION PAGE	READ INSTRUCTIONS BEFORE COMPLETING FORM
1. REPORT NUMBER: NSWC TR 85-244	2. GOVT ACCESSION NO.: AD-A158 693
	3. RECIPIENT'S CATALOG NUMBER:
4. TITLE *(and Subtitle)*: EMITTANCE MEASUREMENTS OF SPACE CHARGE DOMINATED ELECTRON BEAM	5. TYPE OF REPORT & PERIOD COVERED: Final
	6. PERFORMING ORG. REPORT NUMBER:
7. AUTHOR(s): WON NAMKUNG AND ERIC P. CHOJNACKI*	8. CONTRACT OR GRANT NUMBER(s):
9. PERFORMING ORGANIZATION NAME AND ADDRESS: Naval Surface Weapons Center (Code R43), 10901 New Hampshire Avenue, Silver Spring, Maryland 20903-5000	10. PROGRAM ELEMENT, PROJECT, TASK AREA & WORK UNIT NUMBERS:
11. CONTROLLING OFFICE NAME AND ADDRESS:	12. REPORT DATE: 1 June 1985
	13. NUMBER OF PAGES: 32
14. MONITORING AGENCY NAME & ADDRESS*(if different from Controlling Office)*:	15. SECURITY CLASS. *(of this report)*: UNCLASSIFIED
	15a. DECLASSIFICATION/DOWNGRADING SCHEDULE:

16. DISTRIBUTION STATEMENT *(of this Report)*

Approved for public release, distribution unlimited.

17. DISTRIBUTION STATEMENT *(of the abstract entered in Block 20, if different from Report)*

18. SUPPLEMENTARY NOTES

*University of Maryland, College Park, Maryland 20742

19. KEY WORDS *(Continue on reverse side if necessary and identify by block number)*

Emittance
Space Charge Dominated Beam

20. ABSTRACT *(Continue on reverse side if necessary and identify by block number)*

A diagnostic technique of the beam emittance is developed for electron beams with diverging envelopes under strong space charge forces. Radial profiles of current density, local temperature, and divergence angle are measured by the slit-pinhole method for axisymmetric beams. The particle distribution function in transverse phase space is then constructed and the rms emittance is obtained by numerical integrations. A 5 kV, 200 mA, and 3 μsec electron beam is used in the comparison between theory and experiment

DD FORM 1 JAN 73 1473 EDITION OF 1 NOV 65 IS OBSOLETE

S/N 0102-LF-014-6601

UNCLASSIFIED

SECURITY CLASSIFICATION OF THIS PAGE *(When Data Entered)*

on this diagnostic method.

FOREWORD

A diagnostic technique of the beam emittance is developed for electron beams with diverging envelopes under strong space charge forces. Radial profiles of current density, local temperature, and divergence angle are measured by the slit-pinhole method for axisymmetric beams. The particle distribution function in transverse phase space is then constructed and the rms emittance is obtained by numerical integrations. A 5 kV, 200 mA, and 3 μsec electron beam is used in the comparison between theory and experiment on this diagnostic method.

We are grateful to Drs. M. J. Rhee, J. Y. Choe, and J. D. Lawson for helpful discussions. This work is supported by the Independent Research Fund at Naval Surface Weapons Center and by the Department of Energy at the University of Maryland.

Approved by:

Ira M Blatstein

IRA M. BLATSTEIN, Head
Radiation Division

CONTENTS

ILLUSTRATIONS

SECTION 1

INTRODUCTION

There are numerous applications of charged particle beams ranging from electron microscopes to high energy particle accelerators. In their various stages of formation, acceleration, transport, and focusing, charged particle beams are commonly required to be of high quality. One of the physical quantities that measure beam quality is the emittance, which is proportional to the phase space area occupied by the beam particles. The emittance is closely related to the brightness in electron microscopy and to transverse temperature in plasma physics.[1] Even though the definition of emittance and its measurement principles are very simple, it is known that experimentally obtaining a meaningful and/or comparable quantity is very difficult. Various methods of emittance measurement[2,3] have been introduced in the past, especially in particle accelerator physics.

In free space, the envelope of a non-neutral charged particle beam expands due to space charge forces and transverse beam emittance. Depending on relative contribution to envelope expansions, one may classify a beam as either space charge dominated or emittance dominated. In the space charge dominated beams, for reasons which will be apparent in Section 3, sample beamlets are distorted so that results from conventional methods are inadequate in representing beam quality.

Recently the emittance changes under the strong influence of space charge forces have been experimentally investigated for electron beams at the University of Maryland.[4] In this experiment one should compare the measured emittances under various conditions. This work[5,6] has been carried out in connection with the University of Maryland electron beam transport experiment, in which a space charge dominated electron beam is transported through a solenoid focusing channel to investigate the emittance growth.

In this paper, briefly reviewing various emittance definitions for practical beams, the slit-pinhole method is introduced to find parameters in constructing the distribution function in transverse phase space for an axisymmetric beam. A low energy electron beam in space charge dominated regime is used to evaluate this diagnostic technique.

SECTION 2

ROOT-MEAN-SQUARE EMITTANCE

When a particle beam propagates along the z-direction, one denotes $f_4(x,p_x,y,p_y)$ as the distribution function in transverse phase space. In the paraxial approximation where p_z is approximated to be constant and far greater than p_x and p_y, the distribution function is conveniently described as $f_4(x,x',y,y')$, where $x' = p_x/p_z = dx/dz$ and $y' = p_y/p_z = dy/dz$. In xx' phase space, the particle distribution is then

$$f_2(x,x') = \iint f_4(x,x',y,y')dydy'. \tag{1}$$

The phase space area occupied by beam particles can be described as

$$A_x = \iint_{f_2 \neq 0} dxdx', \tag{2}$$

and beam emittance is then defined as

$$\varepsilon_x = \frac{A_x}{\pi} \tag{3}$$

Similarly ε_y is defined in yy' phase space. In general, ε_x and ε_y are not the same unless the beam is axisymmetric. One may further define the normalized emittance

$$\varepsilon_{n,x} = \gamma\beta\varepsilon_x \tag{4}$$

as a conserved quantity with respect to changes in p_z such as in an accelerating system.

For most real beams, the phase space area defined in Eq. (2) is unbounded. However, experimental measurements will give a finite value due mainly to instrument resolution. This results in beam quality as measured by emittance is a function of instrument resolution. In addition, the phase space area is often deformed by various nonlinear force effects so that the emittance defined through Eqs. (2) and (3) is inconvenient from the practical point of view.

In order to avoid these difficulties encountered in determining phase space area, a root-mean-square(rms) emittance is introduced, especially, in particle accelerator physics. The rms emittance $\bar{\varepsilon}_x$ is defined[1] as

$$\bar{\varepsilon}_x = 4\,[\,\langle x^2\rangle\langle x'^2\rangle - \langle xx'\rangle^2\,]^{1/2}, \tag{5}$$

where, $\langle\ \rangle$ denotes an average value over $f_2(x,x')$ distribution. We also define $f_1(x)$, and $f_1(x')$ as

$$f_1(x) = \int f_2(x,x')dx', \tag{6}$$

and

$$f_1(x') = \int f_2(x,x')dx. \tag{7}$$

One should note that $f_1(x)$ and $f_1(x')$ are particle distributions projected onto the x- and x'-coordinates. An ideal particle distribution

function called the Kapchinskij-Vladimirskij (K-V) distribution,[1] is often used for theoretical studies. In this distribution, particle distribution projected onto any two dimensional space is uniform, and beam emittance ε_x is the same as rms emittance $\bar{\varepsilon}_x$ defined in Eq. (5). The rms emittance is, therefore, used in comparison between a real beam and the corresponding ideal beam.

In real beam cases, the distribution function $f_2(x,x')$ is graphically expressed by equidensity contour lines in the xx' plane. These contour lines are, in general, ellipses with major axis tilted with respect to the coordinate axis. In a special case, where the major axis coincides with the coordinate axis, i.e., in upright ellipse case, Eq. (5) becomes

$$\bar{\varepsilon}_x = 4 \langle x^2 \rangle^{1/2} \langle x'^2 \rangle^{1/2} = 4 \bar{x} \bar{x}'. \tag{8}$$

Eq. (8) implies that it is sufficient to know $f_1(x)$ and $f_1(x')$ to determine rms emittance of a beam. This case of an upright ellipse occurs at extrema of the beam envelope along the z-axis. The envelope maximum point may not be accessible due to the fact that it occurs at the lens center. The minimum point is not a practical choice since the sampling points are dramatically reduced or the waist is not often predicted. Thus, emittance measurements are usually done on a diverging or converging beam.

SECTION 3

SLIT-PINHOLE METHOD FOR SPACE CHARGE DOMINATED BEAM

The distribution function $f_2(x,x')$ can be measured by employing a pair of long slits separated by a proper axial distance. The first slit plane stops most of the beam particles except those with the same x value of the slit. The second slit is then scanned along x direction in order to obtain $f_2(x,x')$ at the given x value. Repeating this at other x values, one can scan the particle distribution in whole xx' space. In this procedure, one has to keep the slits parallel. This is very difficult experimentally. In addition, there arises another difficulty; when the beam particle distribution is not uniform in real space, the sample beamlet passing the first slit plane bends like an arc due to nonlinear diverging forces. The particles detected by the second slit due to this bending effect can not be distinguished experimentally from that of the velocity distribution. Therefore, the slit-slit method is not an adequate one for space charge dominated beams. When one employs a small-pinhole moving along the x-axis instead of the second slit, these difficulties, i.e., alignment and beamlet bending will be overcome. The phase space distribution measured in this way is not the same to the one defined in Eq. (1). Therefore, we discuss the procedure in obtaining the rms emittance in the slit-pinhole method.

Consider an axisymmetric beam with an envelope diverging in free space under its own space charge forces. Assume further that the local

temperature $T_\perp(r)$ represents the Maxwell-Boltzmann velocity distribution. We may then restate the assumptions without loss of generality as follows:

1. The particle density distribution in real space is a radial function $n(r)$.

2. The beam diverges radially, i.e., a cylindrical shell of radius r in the beam diverges with a slope $\eta(r)$.

3. The transverse temperature is also a radial function $T_\perp(r)$. It is conveniently described as $\sigma(r) = (kT_\perp(r)/mv_o^2)^{1/2}$, where k is the Boltzmann constant and v_o is the axial velocity of the particles. The distribution function of the beam in transverse phase space can be written as

$$f_4(x,x',y,y') = n(r)\left[\frac{1}{2\pi\sigma^2}\, e^{-(x'-\eta_x)^2/2\sigma^2}\, e^{-(y'-\eta_y)^2/2\sigma^2}\right] \tag{9}$$

where, $\eta_x = \eta(r)x/r$, $\eta_y = \eta(r)y/r$, and $n(r)$ is a normalized radial density distribution function satisfying

$$2\pi\int_0 n(r)rdr = 1. \tag{10}$$

When $n(r)$, $\eta(r)$, and $\sigma(r)$ are measured experimentally, $f_2(x,x')$ can be obtained by analytical and/or numerical integration of f_4 over y and y'. The slit-pin hole method can be used to obtain these parameters.

The diagnostic arrangement for the slit-pinhole system is schematically shown in Figure 1. The slit plane is located at z = 0 with a narrow slit parallel to the y-axis. A sheet beamlet passes through the slit of width 2d and the diverging beamlet profile is scanned by a current (particle) collector in the screen plane z = L. The current collector is covered by a plate with a pinhole of radius r_p which travels on the ξ-axis, This system is commonly

designed as L > a (beam radius) >> d > r_p that the side dimension of the sheet beamlet spreads due mainly to the transverse temperature of the beamlet.

When the slit is located at $x = x_o$, the density n_p detected by a pinhole collector on the ξ-axis, i.e., $\zeta = 0$, becomes

$$n_p(\xi;x_o) = \int_{-\infty}^{\infty} dy \int_{-\infty}^{\infty} dy' \int_{-\infty}^{\infty} dx' \int_{x_o-d}^{x_o+d} dx\, f_4(x,x',y,y')\left(\frac{1}{L^2}\right)\delta\left(x'-\frac{\xi-x}{L}\right)\delta\left(y'+\frac{y}{L}\right) \quad (11a)$$

$$= \frac{d}{\pi L^2}\int dy\, \frac{n}{\sigma^2}\, e^{-(\xi-x_o+\eta_x L)^2/2\sigma^2L^2} e^{-(y+\eta_y L)^2/2\sigma^2L^2}, \quad (11b)$$

where the argument for n, η, and σ is $r = (x_o^2 + y^2)^{1/2}$. Here, we have used the condition that the slit opening 2d is very small, $d << \sigma L << a$. The effect of a finite slit width is discussed in the next section.

The last term in Eq. (11) is a monotonically decreasing even function of y from its peak value at y = 0. When $\sigma L << 1$, it can also be approximated as

$$e^{-(y+\eta_y L)^2/2\sigma^2L^2} \xrightarrow{\sigma L<<1} \sqrt{2\pi}\,\sigma L\,\delta(y). \quad (12)$$

Substituting Eq. (12) into Eq. (11), we obtain

$$n_p(\xi;\, x_o) \simeq \frac{2d}{\sqrt{2\pi}\,L}\,\frac{n(x_o)}{\sigma(x_o)}\, e^{-(\xi-x_o+\eta L)^2/2\sigma^2L^2} \quad (13)$$

Therefore, n(r), η(r), and σ(r) can be obtained from Eq. (13). The beamlet profile $n_p(\xi;x_o)$ is a gaussian with a peak value proportional to $n(x_o)/\sigma(x_o)$, the peak shift ηL, and the rms width σL. This relationship is shown in Figure 2. One notes that we should integrate Eq. (13) to obtain $n(x_o)$ unless $\sigma(x_o)$ is constant throughout the beam cross section.

SECTION 4

FINITE SLIT WIDTH EFFECT

In order to see the finite slit effect of the sheet beamlet profile on the screen, let us consider an one-dimensional sheet beam: A sheet beam of uniform density n_o and thickness 2d is located on the y-axis. Let us assume that the velocity space distribution is a Maxwellian with a temperature T and the beam (current) density is so small that we can neglect the space charge broadening of the sheet beam. The density distribution in the screen plane $z = L$ is then expressed as

$$n(\xi) = \frac{n_o}{\sqrt{2\pi}\,\sigma L} \int_{-d}^{d} e^{-(\xi-x)^2/2\sigma^2L^2}\, dx \tag{14a}$$

$$= \frac{n_o}{2}\left[\mathrm{erf}\left(\frac{|\xi|+d}{\sqrt{2}\sigma L}\right) - \mathrm{erf}\left(\frac{|\xi|-d}{\sqrt{2}\sigma L}\right)\right], \tag{14b}$$

where

$$\mathrm{erf}(x) = \frac{2}{\sqrt{\pi}} \int_{0}^{x} e^{-t^2}\, dt \tag{15}$$

is the error function. $n(\xi)$ is peaked at $\xi = 0$ and it is a decreasing even function of ξ. The profile shape is characterized by three parameters; d, σ, and L.

When $d << \sigma L$, Eq. (14a) can be approximated as

$$n(\xi) \simeq \frac{n_o}{\sqrt{2\pi}\sigma L} e^{-\xi^2/2\sigma^2 L^2} \left(\frac{\sigma^2 L^2}{\xi}\right) 2 \sinh \left(\frac{\xi d}{\sigma^2 d^2}\right) \qquad (16a)$$

$$\simeq \frac{n_o}{\sqrt{2\pi}\sigma L} e^{-\xi^2/2\sigma^2 L^2} (2d), \qquad \text{for } |\xi| < d. \qquad (16b)$$

One can readily see that Eq. (16b) is also valid for $\xi >> d$.

For cases where $d \approx \sigma L$ one needs numerical calculations for $n(\xi)$. As examples, $n(\xi)$ is plotted for various $(\sigma L/d)$ values in Figure 3. One should maintain $\sigma L/d > 0.4$ to avoid a flat top distribution in $n(\xi)$. However, one should note that a peaked profile is not a sufficient condition for diagnostics of the beam temperature, as evident from Figure 3. The rms width of the profile should be larger than d.

Since σ is an unknown quantity to be measured, L/d is a more convenient quantity for the system design. Therefore, in order for the profile to represent the velocity distribution of a sheet beam, the parameter (L/d) should be very large, since $\sigma << 1$ On the other hand, d is governed by the fact that the density should be uniform across the slit opening, and r_p is small enough to detect many data points over σL.

SECTION 5

DESCRIPTION OF EXPERIMENTAL APPARATUS

A schematic of the electron beam transport channel at the University of Maryland is shown in Figure 4, where the beam emittance measurement has been conducted. An electron beam is produced by a converging Pierce-type gun with a cathode radius R_c = 1.27 cm. The gun is typically operated at 5 kV, 200-220 mA, 3 μsec pulse length, and 60 Hz repetition rate. In the first phase of the 40 period experiment,[7] there are 14 solenoidal focusing lenses of which the first two, M1 and M2, are independently controlled for matching the beam into the channel of periodically spaced lenses, C1 to C12. The system vacuum is maintained at < 1 X 10^{-7} Torr by a 400 ℓ /sec turbo-molecular pump and two 8 ℓ /sec ion pumps.

The slit-pinhole system for emittance measurements is located in the main diagnostic chamber at the end of the channel. The slit is constructed from 0.05 mm thick tantalum foil and the slit opening is 2d = 0.25 mm. The Faraday cup assembly is covered by a tantalum foil with a pinhole of diameter $2r_p$ = 0.1 mm. The inner cup is shaped to minimize secondary electron effects. The cup assembly is mounted on an XYZ manipulator for precise scanning of beamlet profiles. The slit-pinhole separation is L = 86.14 mm so that L/d = 345. This corresponds to σL/d > 2.0 for a 5 keV beam generated in the cathode temperature T_c = 1400°K.

SECTION 6

EMITTANCE MEASUREMENT OF SPACE CHARGE DOMINATED ELECTRON BEAM

A 5 keV, 200 mA, 3 μsec electron beam is transported through the periodic channel. For a given channel focusing strength B_{ch} = 83 G, which corresponds to the phase shift per period in the betatron oscillation is $\sigma_o = 70^o$. The matched beam is obtained by adjusting M1 and M2, and by monitoring the beam radius at the intermediate diagnostic chambers, i.e., between M2 and C1, and C6 and C7. It is independently confirmed by monitoring the beam envelope beyond C11.[6] At the entrance of the main diagnostic chamber, the slit is scanned across the beam while the profile is monitored by the pinhole/Faraday cup.

A typical beamlet profile is shown in Figure 5 along with the best fit gaussian profile in the solid curve. In this case, the measured σ is 4.18 mRad, which corresponds to a transverse temperature $T_\perp = 2027^o$ K. Experimental results for n(r), n(r), and σ(r) are plotted in Figure 6. We obtain $f_2(x,x')$, using Eq. (9) and integrating over y and y'. This is also plotted in equidensity contours, i.e., emittance diagram, in Figure 7. The $f_1(x)$ and $f_1(x')$ are also shown in Figures 8 and 9.

We obtain $\bar{x}$ = 7.09 mm, $\bar{x}'$ = 50.0 mRad, and $\langle xx' \rangle$ = 352.9 mm-mRad. Therefore, the rms-emittance of the beam is 1.34×10^{-4} Meter-Radian. It may be compared to the theoretical value 9.2×10^{-5} Meter-Radian for an electron beam from a planar diode of radius 1.27 cm operated 5 kV and 1400^oK, i.e.,

$$\bar{\varepsilon} = a \sqrt{\frac{2kT_c}{eV}} \qquad (17)$$

where eV is the beam energy.[1,4]

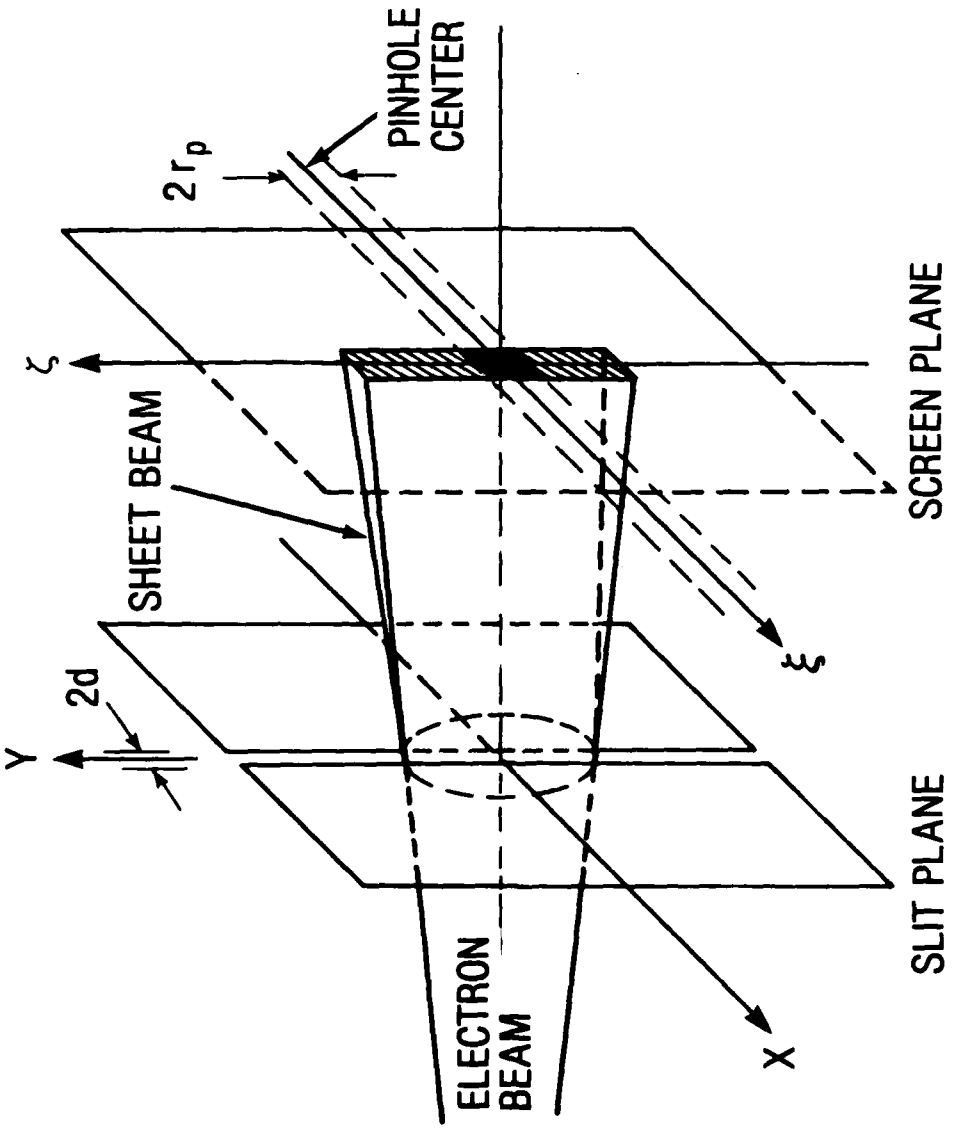

FIGURE 1. SCHEMATIC OF THE SLIT-PINHOLE METHOD FOR BEAM EMITTANCE MEASUREMENTS

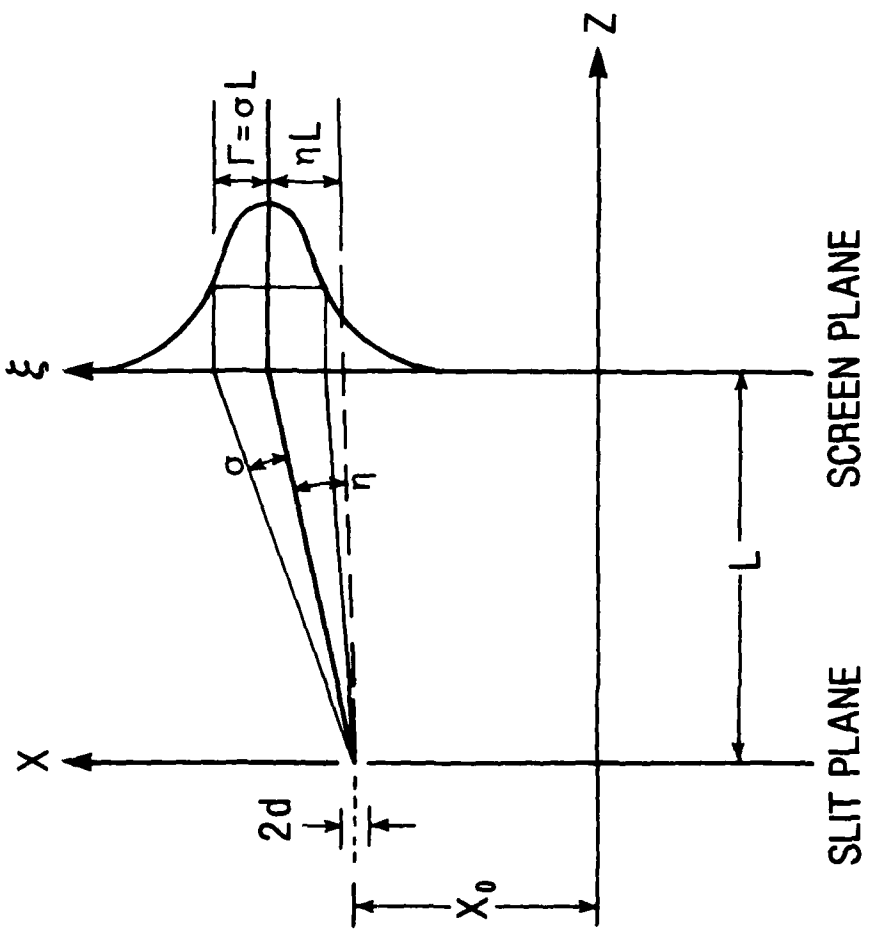

FIGURE 2. GEOMETRY OF THE SLIT-PINHOLE METHOD IN THE X-Z PLANE

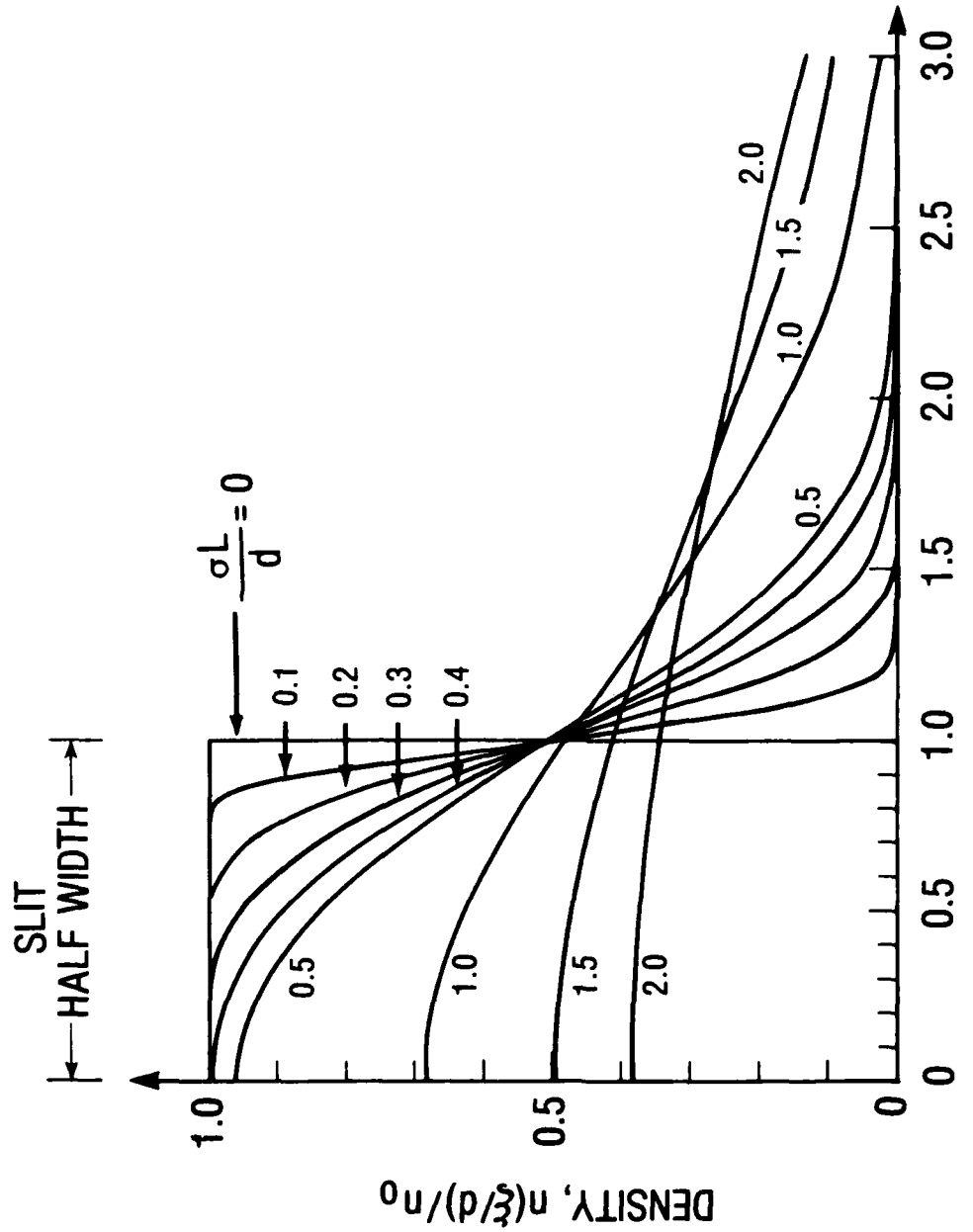

FIGURE 3. DENSITY PROFILES OF A SHEET BEAM WITH THE FINITE SLIT WIDTH; d IS THE HALF WIDTH OF THE SLIT AND L IS THE DISTANCE BETWEEN THE SLIT AND THE SCREEN

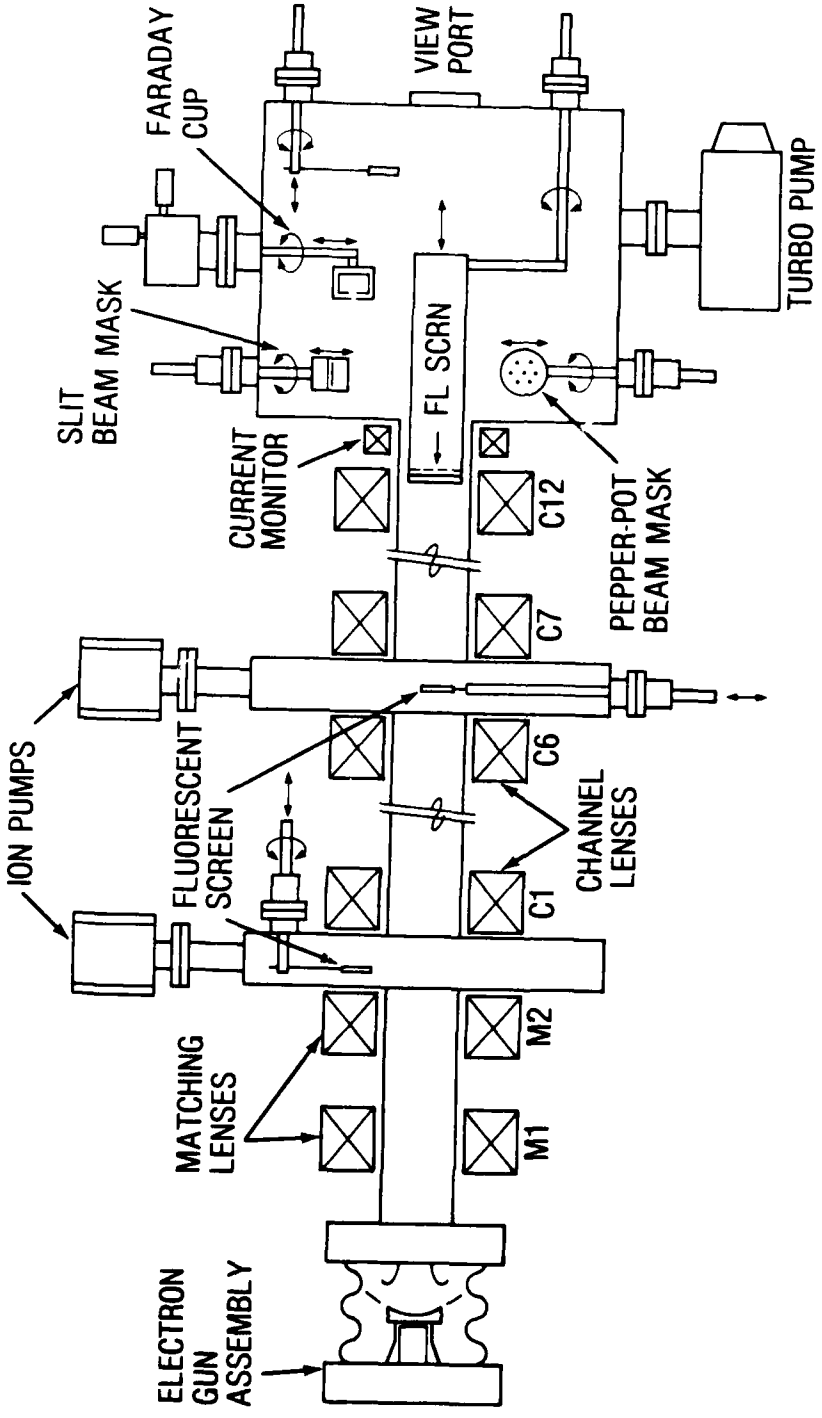

FIGURE 4. SCHEMATIC OF THE ELECTRON BEAM TRANSPORT EXPERIMENT AT THE UNIVERSITY OF MARYLAND

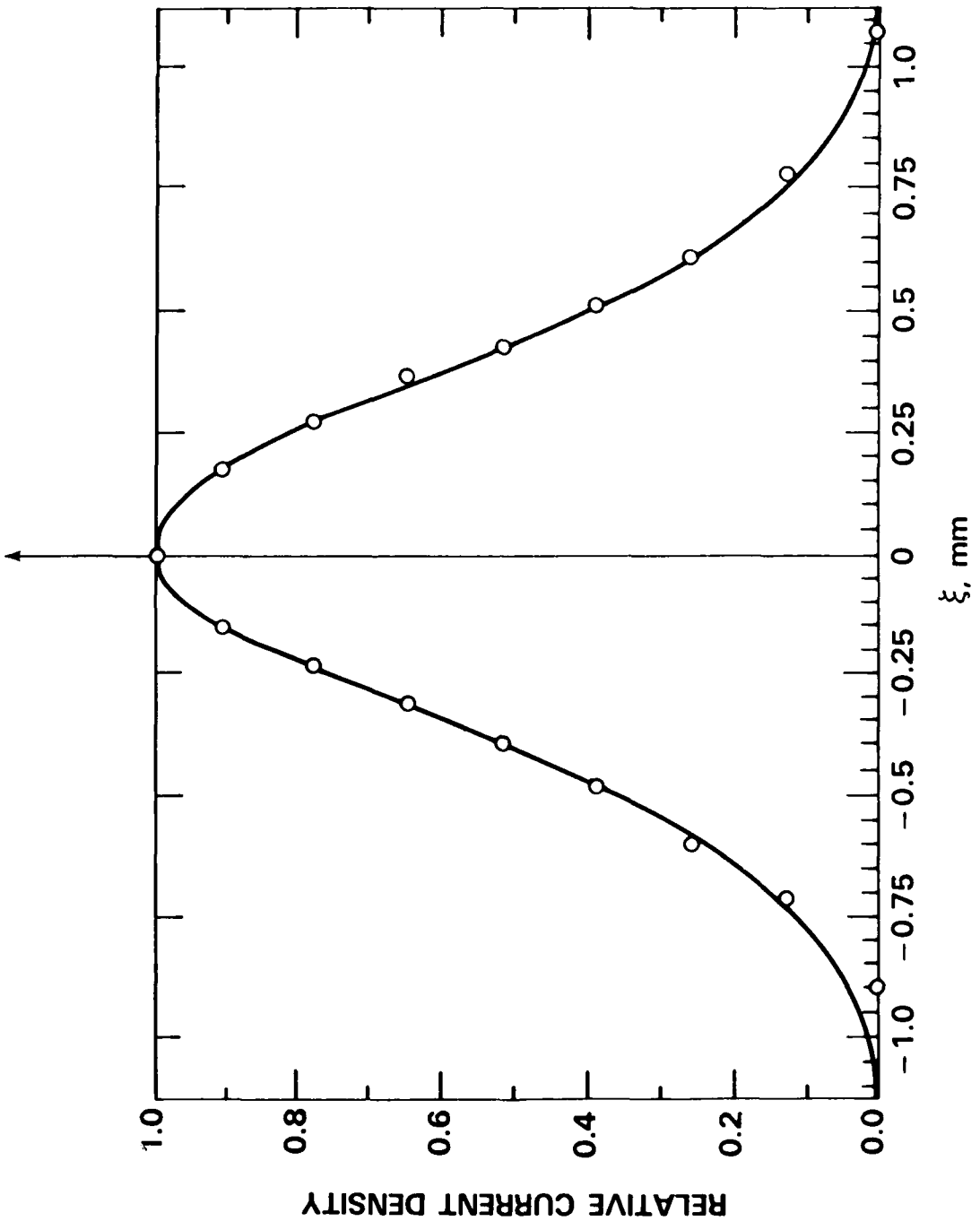

FIGURE 5. TYPICAL BEAMLET PROFILE IN THE SLIT-PINHOLE MEASUREMENT

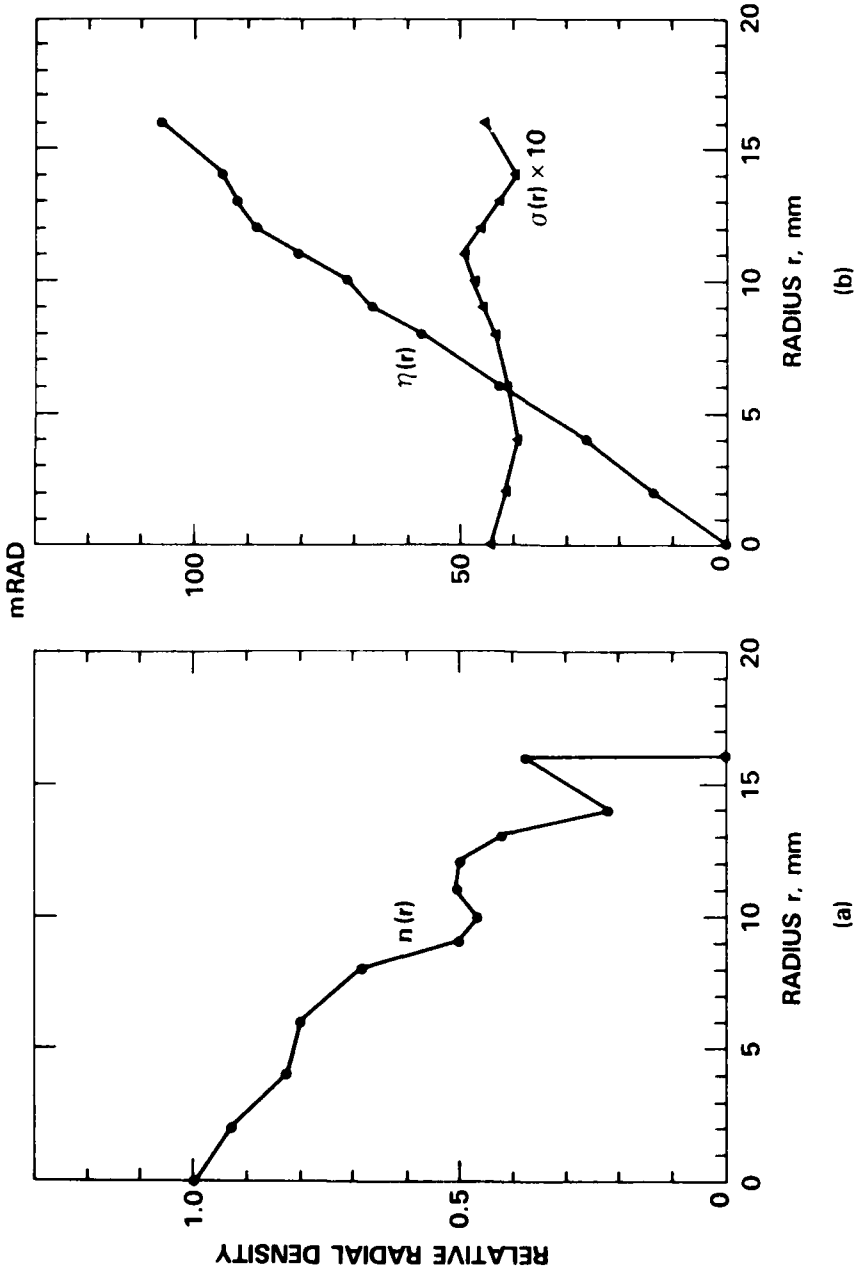

FIGURE 6. BEAM DENSITY n(r), DIVERGING ANGLE η(r), AND TRANSVERSE TEMPERATURE σ(r) FOR A 5 keV, 200 mA ELECTRON BEAM TRANSPORTED THROUGH THE PERIODIC FOCUSING CHANNEL

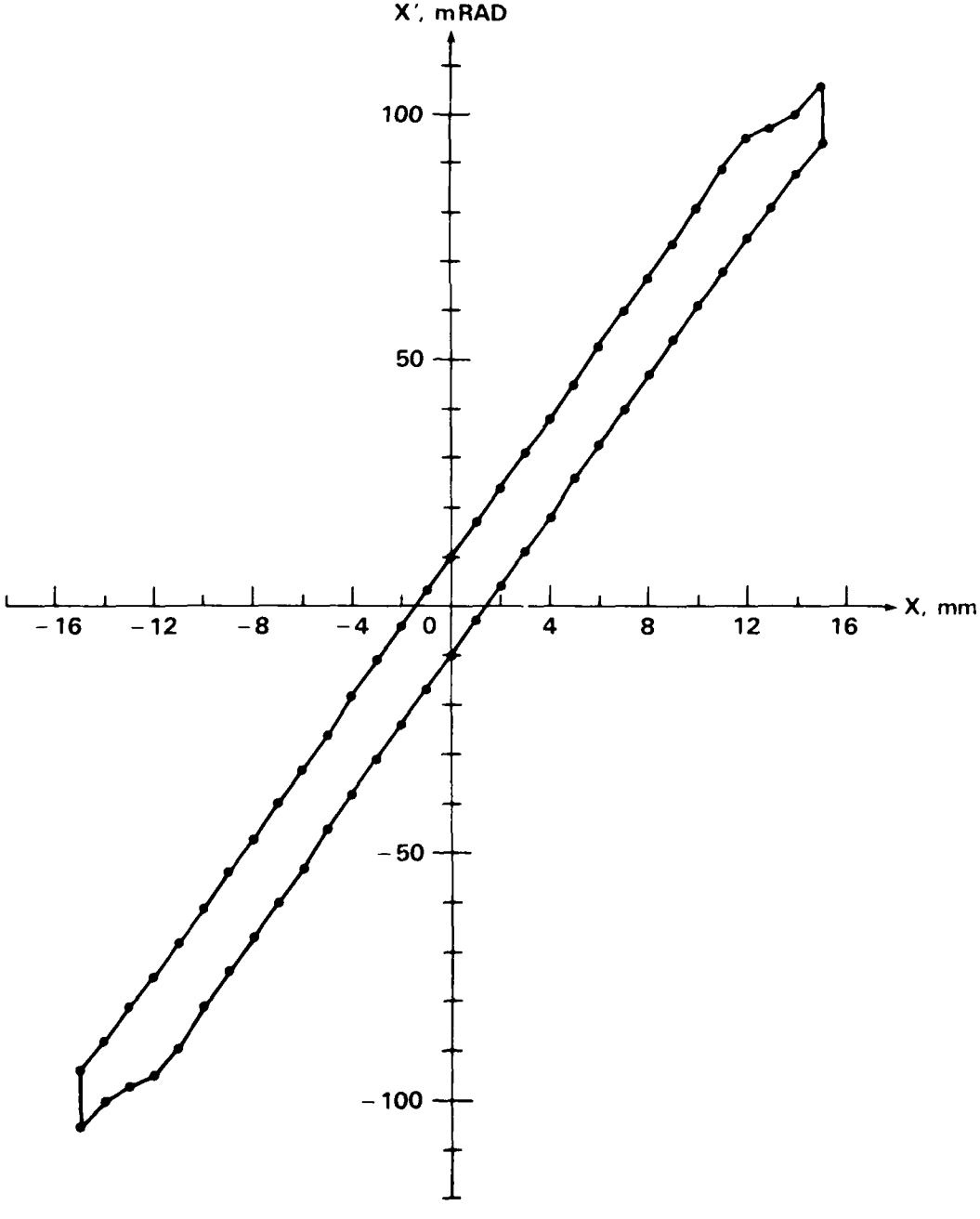

FIGURE 7. EMITTANCE DIAGRAM OF THE ELECTRON BEAM. THE CONTOUR LINE REPRESENTS EQUIDENSITY OF $f_2(x,x') = 0.1\ f_2(0,0)$

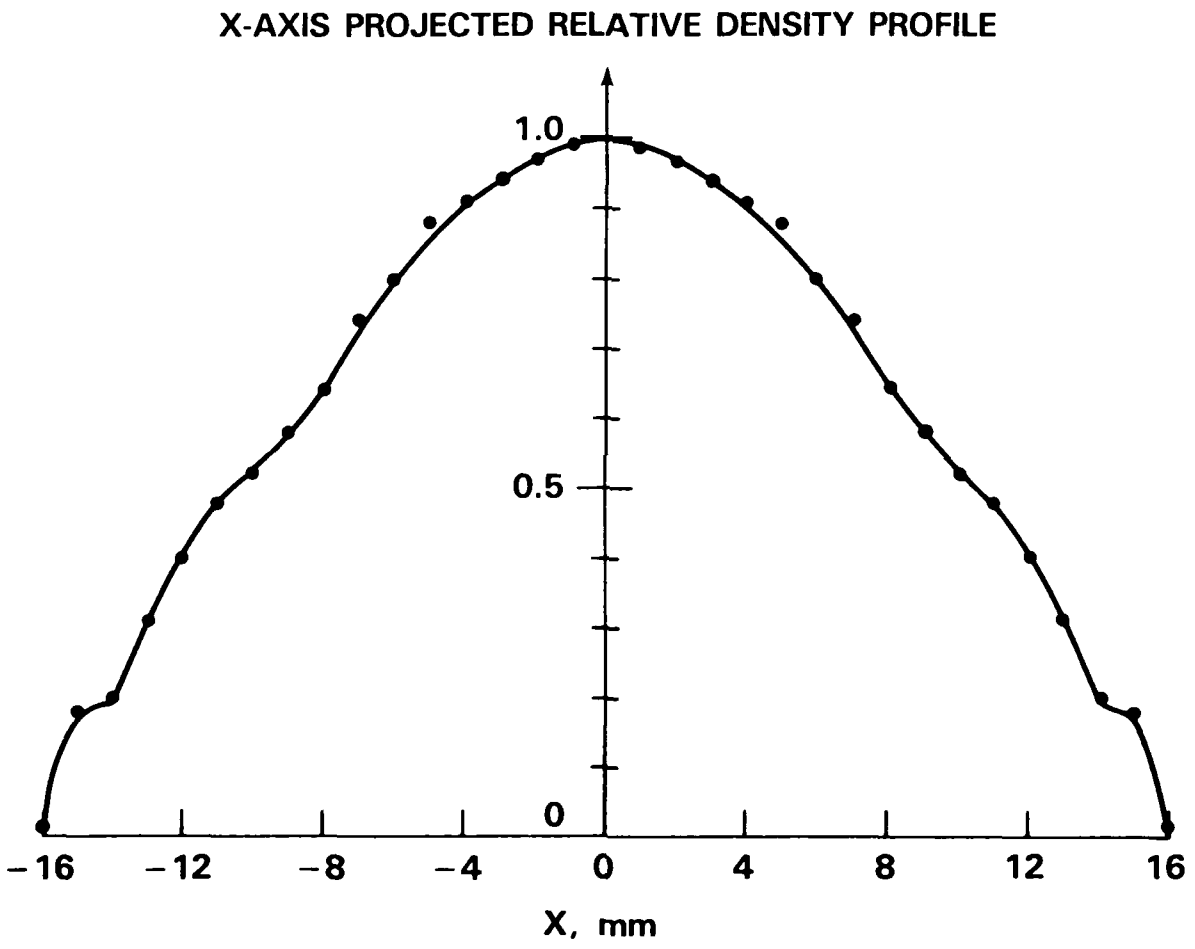

FIGURE 8. DENSITY PROFILE PROJECTED ON THE X-AXIS

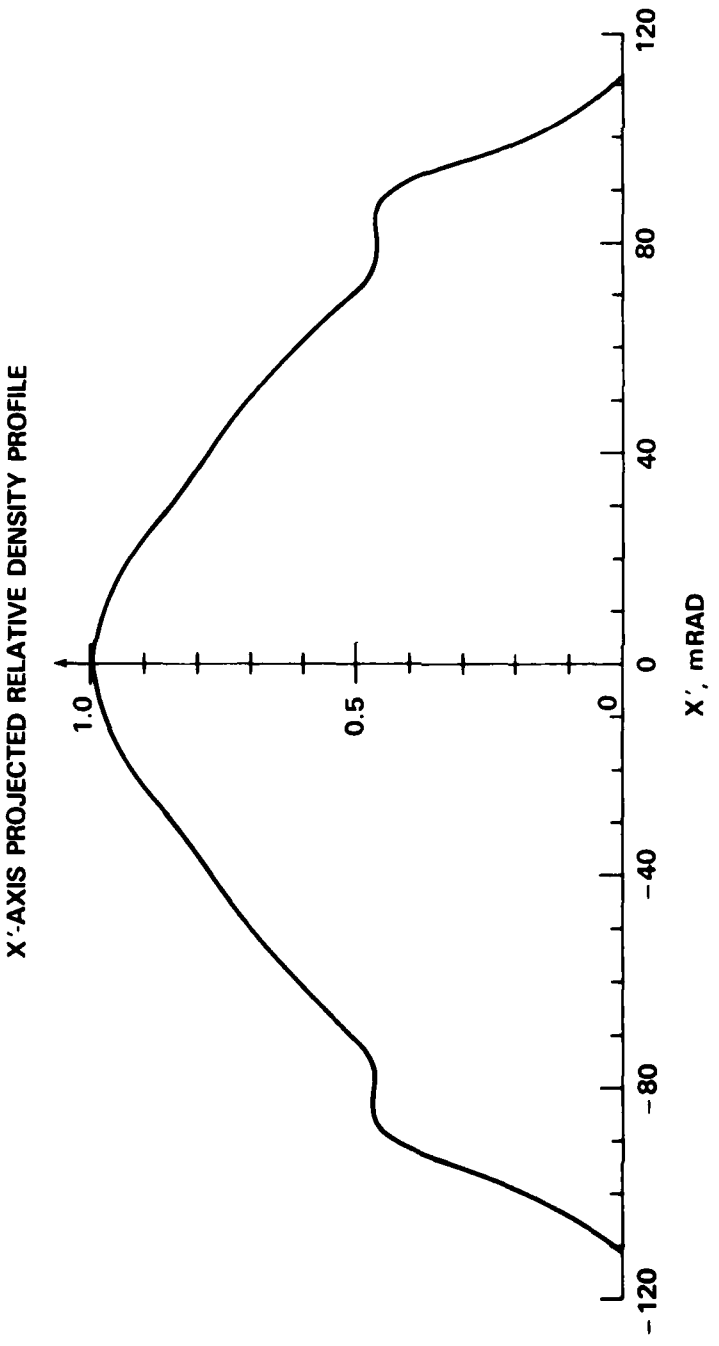

FIGURE 9. DENSITY PROFILE PROJECTED ON THE X' AXIS

REFERENCES

1. Lawson, J. D., The Physics of Charged-Particle Beams (Clarendon, Oxford, 1977), Chapter 4, p. 172.

2. Van Steenbergen, A., Nucl. Instru. Methods 51, 245(1967).

3. Lejeune, A. and Aubert, J., in Applied Charged Particle Optics, Part A. edited by A. Septier (Academic, New York, 1980), p. 159, and references therein.

4. Namkung, W., Loschialpo, P., Reiser, M., Suter, J., and Lawson, J. D. IEEE Trans. Nucl. Sci. NS-28, 2519 (1981).

5. Suter, J., Namkung, W., Chojnacki, E., Loschialpo, P., Reiser, M. and Lawson, J. D.,Bull. Am. Phys. Soc. 27, 981 (1982).

6. Chojnacki, E., Namkung, W., P. Loschialpo, P., McAdoo, J., Reiser, M. and Lawson, J. D., Bull. Am. Phys. Soc. 29, 1432 (1984).

7. Reiser, M., Chojnacki, E., Loschialpo, P., Namkung, W., Lawson, J. D., Proir, C. and Warner, G. P., in Proc. 1984 Linear Acc. Conf., GSI, Darmstadt, W. Germany, GSI-84-11 (1984), p. 309.

DISTRIBUTION

	Copies
Office of the Secretary of Defense Washington, DC 20302-7100	1
Chief Office of Naval Research Attn: Dr. C. W. Roberson Arlington, VA 22217	1
Commander Naval Research Laboratory Attn: Code 6840 (Dr. S. Ahn)	1
Code (Dr. J. Golden)	1
Code 4763 (Dr. R. Greig)	1
Code 4790 (Dr. I. Haber)	1
Code (Dr. C. A. Kapetanakos)	1
Code (Dr. P. Loschialpo)	1
Code (Dr. R. Parker	1
Code (Dr. J. Pasour)	1
Code 4790 (Dr. P. Sprangle) Washington, DC 20375	1
U. S. Department of Energy Division High Energy Physics Attn: Dr. R. Sah (MS-ER-22-GTN)	1
Dr. D. Sutter	1
Office of Inertial Fusion Attn: Dr. T. Godlove Washington, DC 20585	1
National Bureau of Standards Attn: Dr. M. Wilson Gaithersburgh, MD 20760	1
The Pentagon Attn: COL R. Gullickson (SDIO/DEW) Washington, DC 20301	1

	Copies
Lawrence Berkeley Laboratory Attn: Dr. D. Keefe	1
Dr. C. H. Kim	1
Dr. E. P. Lee	1
Dr. L. Smith	1
1 Cyclotron Road Berkeley, CA 94720	
Sandia National Laboratory Division 5246 Attn: Dr. B. R. Mill	1
Albuquerque, NM 87115	
Los Alamos National Laboratory Attn: Dr. L. E. Thode (MS-608)	1
Los Alamos, NM 87758	
Lawrence Livermore Laboratory University of California Attn: Dr. R. Briggs	1
Dr. J. W-K. Mark	1
Dr. V. K. Neil	1
Dr. D. S. Prono	1
Dr. D. Prosnitz	1
Dr. S. Yu	1
Dr. W.A. Barletta (L-321)	1
Livermore, CA 94550	
University of California Laboratory for Plasma Studies Attn: Prof. H. H. Fleischmann	1
Prof. J. Nation	1
Irvine, CA 92664	
Cornell University Attn: Dr. L. E. Thode (MS-608)	1
Attn: Prof. H. H. Fleischmann	1
Ithaca, NY 14850	

DISTRIBUTION (Continued)

	Copies
University of Maryland Electrical Engineering Department Attn: Prof. W. Destler	1
Prof. M. P. Reiser	1
College Park, MD 20742	
University of New Mexico Department of Nuclear Engineering Attn: Prof. S. Humphries, Jr. Albuquerque, NM 87131	1
Massachusetts Institute of Technology Attn: Prof. G. Bekefi Bldg. 36-213 77 Massachusetts Ave. Cambridge, MA 02139	1
Defense Technical Information Center Cameron Station Alexandria, VA 22314	12
Library of Congress Attn: Gift and Exchange Division Washington, DC 20540	4

Internal Distribution	Copies
R	1
R04	1
R40	1
R401	1
R41 (M. Brown)	1
R41 (R. Fiorito)	1
R41 (M. Rhee)	1
R41 (D. Rule)	1
R41 (J. Smith)	1
R41 (R. Schneider)	1
R41 (H. Uhm)	1
R42 (C. Larson)	1
R43 (J.Cunningham)	1
R43 J. Choe)	1
R43 (D. Jablonski)	1
R43 (A. Krall)	1
R43 (W. Namkung)	10
R44 (T. Zien)	1
R45 (H. Riedl)	1
F34 (J. Nolting)	1
E35 (GIDEP Office)	1
E231	9
E232	3


DATE
ILMED
-8